Inorganic Chemistry

Article

pubs.acs.org/IC

Three New Quaternary Actinide Chalcogenides Ba_2TiUTe_7, Ba_2CrUTe_7, and $Ba_2CrThTe_7$: Syntheses, Crystal Structures, Transport Properties, and Theoretical Studies

Jai Prakash,[†] Adel Mesbah,[†,‡] Jessica Beard,[†] Sébastien Lebègue,[§] Christos D. Malliakas,[†] and James A. Ibers*[,†]

[†]Department of Chemistry, Northwestern University, 2145 Sheridan Road, Evanston, Illinois 60208-3113, United States

[‡]ICSM, UMR 5257 CEA/CNRS/UM2/ENSCM, Site de Marcoule—Bât. 426, BP 17171, 30207 Bagnols-sur-Cèze Cedex, France

[§]Laboratoire de Cristallographie, Résonance Magnétique et Modélisations (CRM2, UMR CNRS 7036), Institut Jean Barriol, Université de Lorraine, BP 239, Boulevard des Aiguillettes, 54506 Vandoeuvre-lès-Nancy, France

Supporting Information

ABSTRACT: The three new quaternary actinide chalcogenides Ba_2TiUTe_7, Ba_2CrUTe_7, and $Ba_2CrThTe_7$ have been synthesized. From single-crystal X-ray diffraction studies these isostructural compounds are found to crystallize in a new structure type in space group D_{2h}^{16}—*Pnma* of the orthorhombic system. The structure features $^1_\infty[MAnTe_7^{4-}]$ strips (M = Cr or Ti; An = Th or U) that propagate in the *b*-direction and are separated by Ba cations. An atoms are coordinated to eight Te atoms in a bicapped trigonal-prismatic geometry while M atoms are octahedrally coordinated to six Te atoms. Sharing of the $AnTe_8$ and MTe_6 polyhedra forms $^1_\infty[MAnTe_7^{4-}]$ strips. The presence of the infinite linear Te—Te—Te chains in these compounds makes assignment of oxidation states arbitrary. Resistivity measurements and DFT calculations provide further insight into the properties of these compounds.

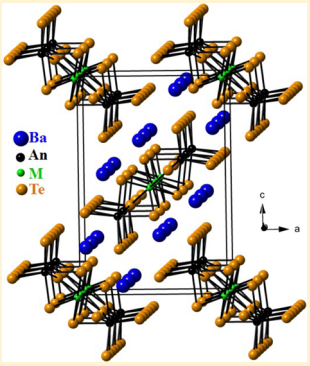

INTRODUCTION

Solid-state actinide chalcogenides often show intriguing phenomena such as superconductivity,[1,2] optical properties,[3−5] charge density waves,[6] and magnetism[3−5] owing to the presence of 5f-electrons. This class of compounds is also important in the field of the nuclear fuel cycle as some metal chalcogenides have potential for selective radioactive waste removal,[7−10] including removal of alkaline-earth metals.[10] The ability of actinides, especially U, to show variable oxidation states (+3, +4 (most common), +5) and the tendency of chalcogens (Q), in particular Te, to form Q—Q interactions often result in unusual crystal structures. Among these actinide chalcogenides, the crystal structures of the tellurides are often more complex because of the ability of Te to form higher order polyanions (as compared with S or Se) such as infinite Te—Te—Te chains or square Te nets. These feature intermediate Te···Te interactions of lengths greater than a Te—Te single bond (2.76 Å) but shorter than a van der Waals interaction (4.10 Å).

The dimensionality of crystal structures of An_xTe_y compounds can be tuned by controlling the An:Te ratio. For example, α-$AnTe_3$ (An = Th,[11] U[12]) adopts a two-dimensional layered crystal structure whereas that of UTe_2[13] is three-dimensional; both structures have the bicapped trigonal $AnTe_8$ prism as a basic building block. In ternary tellurides $A_xAn_yTe_z$ (A = alkali-metal or alkaline-earth metal), electropositive A cations strongly influence dimensionality of the crystal structures. Examples of two-dimensional crystal structures include $CsAn_2Te_6$ (An = Th[14] and U[15]), KTh_2Te_6,[16] and $BaAnTe_4$[17] with infinite Te—Te—Te chains having a nonintegral average charge on each Te. Both $CsUTe_6$[18] and $BaUTe_6$[17] of the 116-family have one-dimensional crystal structures with U/Te chains separated by Cs^{1+} and Ba^{2+} cations, respectively. The connectivity and geometry of actinide polyhedra in these $A_xAn_yTe_z$ compounds are similar to those in the binary An_xTe_y compounds. In contrast, the structures of the $An_xM_yTe_z$ compounds (M = transition metal) comprise the sharing of actinide and transition-metal polyhedra. Examples include $Cu_xAn_2Te_6$ (An = Th[19] and U[20]) and $MnThTe_3$[21] that comprise $AnTe_8$ bicapped trigonal prisms and $CuTe_4$ tetrahedra or $MnTe_8$ octahedra.

The structures of the relatively few known quaternary actinide tellurides are even more varied and range from the simple layered ones of $AAuUTe_3$ (A = Rb, Cs)[22] to the complex three-dimensional ones of $ATiU_3Te_9$ (A = Rb, Cs).[23] To the best of our knowledge there were no examples known of quaternary compounds in the alkaline-earth metal system Ak/An/M/Te, and hence we have carried out exploratory syntheses in this system to discover new compounds. These syntheses have afforded the three new quaternary compounds Ba_2TiUTe_7,

Received: February 11, 2015
Published: March 23, 2015

DOI: 10.1021/acs.inorgchem.5b00338
Inorg. Chem. 2015, 54, 3688−3694

Ba_2CrUTe_7, and $Ba_2CrThTe_7$. Here we present their syntheses, crystal structures, resistivities, and electronic properties.

EXPERIMENTAL METHODS

Syntheses. ***Caution!*** *^{232}Th and ^{238}U are α-emitting radioisotopes and as such are considered a health risk. Their use requires appropriate infrastructure and personnel trained in the handling of radioactive materials.*

The following reactants were used as obtained: Ba (Johnson Matthey, 99.5%), Th (MP Biomedicals, 99.1%), Te (Aldrich, 99.8%), Ti (Alfa, 99.5%), and Cr (Alfa Aesar, 99.99%). Depleted U powder was obtained by hydridization and decomposition of turnings (IBI Laboratories) in a modification[24] of a previous literature method.[25]

All the reactions were performed in sealed 6 mm carbon-coated fused-silica tubes. Chemical manipulations were performed inside an Ar-filled drybox. The reactants were weighed and transferred into tubes that were then evacuated to 10^{-4} Torr, flame-sealed, and placed in a computer-controlled furnace. The tubes were heated to 1173 K in 48 h, annealed for 192 h, and then cooled to 973 K in 99 h followed by cooling to 573 K in 99 h, and finally the furnace was turned off. Semiquantitative EDX analyses of the products of the reactions were obtained with the use of a Hitachi S-3400 SEM microscope.

Synthesis of Ba_2TiUTe_7. The reactants were Ba (34.61 mg, 0.252 mmol), U (10 mg, 0.042 mmol), Ti (4 mg, 0.08 mmol), and Te (85.8 mg, 0.672 mmol). The reaction product contained black needle-shaped crystals of Ba_2TiUTe_7 (Ba:Ti:U:Te ≈ 2:1:1:7), block shaped crystals of BaTe (Ba:Te ≈ 1:1), TiTe (Ti:Te ≈ 1:1), and black plates of UOTe.[26]

Synthesis of Ba_2CrUTe_7. The reactants were Ba (34.61 mg, 0.252 mmol), U (10 mg, 0.042 mmol), Cr (4.4 mg, 0.084 mmol), and Te (85.8 mg, 0.672 mmol). The reaction product contained black needle-shaped crystals of Ba_2CrUTe_7 (Ba:Cr:U:Te ≈ 2:1:1:7), block shaped crystals of BaTe (Ba:Te ≈ 1:1), CrTe (Cr:Te ≈ 1:1), and black plates of UOTe.[26]

Synthesis of $Ba_2CrThTe_7$. The reactants were Ba (35.50 mg, 0.259 mmol), Th (10 mg, 0.043 mmol), Cr (4.5 mg, 0.087 mmol), and Te (88.0 mg, 0.690 mmol). The reaction product contained black needle-shaped crystals of $Ba_2CrThTe_7$ (Ba:Cr:Th:Te ≈ 2:1:1:7), block shaped crystals of BaTe (Ba:Te ≈ 1:1), CrTe (Cr:Te ≈ 1:1), and black plates of ThOTe.[27]

Structure Determinations. The crystal structures of all three compounds were determined from single-crystal X-ray diffraction data collected with the use of graphite-monochromatized Mo Kα radiation (λ = 0.71073 Å) at 100(2) K on a Bruker APEX2 diffractometer.[28] The algorithm COSMO implemented in the program APEX2 was used to establish the data collection strategy with a series of 0.3° scans in ω and φ. The exposure time was 15 s/frame, and the crystal-to-detector distance was 60 mm. The collection of intensity data as well as cell refinement and data reduction were carried out with the use of the program APEX2.[28] Face-indexed absorption, incident beam, and decay corrections were performed with the use of the program SADABS.[29] Precession images of the data sets provided no evidence for modulation or supercells. All structures were solved and refined in a straightforward manner with the use of the SHELX14 programs.[29,30] The program STRUCTURE TIDY[31] in PLATON[32] was used to standardize the atomic positions. Further details are given in Table 1 and in the Supporting Information.

Resistivity Studies. Four-probe resistivity data were collected between 300 and 500 K using equipment and procedures described previously.[17,33] The dc current was applied along an arbitrary direction on each single crystal.

Theoretical Calculations. To perform our ab initio calculations, we have used the Vienna ab Initio Simulation Package[34,35] implementing density functional theory (DFT)[36,37] with the projector augmented wave method.[38] The Heyd−Scuseria−Ernzerhof (HSE) functional[39−41] was used as the exchange-correlation potential, and spin-polarization was allowed. The geometries (atom positions and cell parameters) were taken identical to the experimental values. For $Ba_2CrThTe_7$ and Ba_2TiUTe_7, the different magnetic orders possible in a crystallographic cell were calculated, and the configuration with the lowest total energy was retained as the ground state. A *k*-point mesh of 2 × 4 × 2 to sample the Brillouin zone and the default cutoff for the plane-wave part of the wave function were used. Calculations for Ba_2CrUTe_7 were not attempted because of the large number of possible magnetic arrangements.

Table 1. Crystallographic Data and Structure Refinement Details for Three Members of the Ba_2MAnTe_7 Family[a]

	Ba_2TiUTe_7	Ba_2CrUTe_7	$Ba_2CrThTe_7$
a (Å)	12.4970(2)	12.4711(3)	12.5766(2)
b (Å)	6.1430(1)	6.1653(1)	6.2297(1)
c (Å)	18.5883(1)	18.5645(4)	18.7183(4)
V (Å^3)	1426.99(4)	1427.39(5)	1466.55(5)
ρ (g cm^{-3})	6.767	6.784	6.576
μ (mm^{-1})	31.277	31.470	29.730
$R(F)^b$	0.019	0.019	0.016
$R_w(F_o^2)^c$	0.043	0.043	0.027

[a]For all structures, space group is D_{2h}^{16}−*Pnma*, λ = 0.71073 Å, *T* = 100(2) K, *Z* = 4. [b]$R(F) = \Sigma||F_o| - |F_c||/\Sigma|F_o|$ for $F_o^2 > 2\sigma(F_o^2)$. [c]$R_w(F_o^2) = \{\Sigma[w(F_o^2 - F_c^2)^2]/\Sigma wF_o^4\}^{1/2}$. For $F_o^2 < 0$, $w^{-1} = \sigma^2(F_o^2)$; for $F_o^2 \geq 0$, $w^{-1} = \sigma^2(F_o^2) + (qF_o^2)^2$ where $q = 0.0177$ for Ba_2TiUTe_7, 0.0250 for Ba_2CrUTe_7, and 0.0070 for $Ba_2CrThTe_7$.

RESULTS AND DISCUSSION

Syntheses. By the reaction of the elements at 1173 K the compounds Ba_2TiUTe_7, Ba_2CrUTe_7, and $Ba_2CrThTe_7$ were obtained in yields of about 30, 30, and 20 wt %, respectively, based on An. Byproducts were MTe (M = Cr, Ti), BaTe, and AnOTe. The approximate amounts of the latter were 20−30 wt %. The actinides are very oxyphilic. Even though the silica tubes were carbon-coated, etching occurred leading to the formation of these AnOTe compounds. Further attempts to improve the yields of Ba_2TiUTe_7 and Ba_2CrUTe_7 by loading stoichiometric amounts of elements with NaI flux failed. No attempt was made to improve the yield for $Ba_2CrThTe_7$. The relatively small yields of desired products coupled with our inability to remove diverse magnetic byproducts precluded our performing magnetic measurements on these materials.

Crystal Structures. The isostructural compounds Ba_2TiUTe_7, Ba_2CrUTe_7, and $Ba_2CrThTe_7$ crystallize in a new structure type with four formula units in space group D_{2h}^{16}−*Pnma* of the orthorhombic crystal system. Crystallographic details on these compounds are presented in Table 1 and in Supporting Information. The asymmetric unit of the structure comprises one An atom (site symmetry *.m.*), two Ba atoms (*.m.*), one M atom ($\bar{1}$), and five Te atoms (Te1(1), Te2(1), Te3(*.m.*), Te4(*.m.*), and Te5(*.m.*)). The unit cell of Ba_2MAnTe_7 is shown in Figure 1. Each An atom in this structure is coordinated to eight Te atoms in a bicapped trigonal-prismatic fashion, and each M atom is octahedrally coordinated to six Te atoms. Each $AnTe_8$ polyhedron shares a Te5 atom with its two neighbors (Figure 2A), and each MTe_6 octahedron edge- and corner-shares with $AnTe_8$ polyhedra (Figure 2B). The resultant structure comprises isolated one-dimensional $^1_\infty[MAnTe_7^{4-}]$ strips that propagate in the *b*-direction and are separated by Ba atoms. The thickness and height of these strips in the three compounds are about 4.2−4.3 and 10.3−10.5 Å, respectively. Figure 3 shows the various similarities among the crystal structures of Ba_2MAnTe_7, α-$AnTe_3$,[11,12] UTe_2,[13] and $CsTiUTe_5$.[18] The structure of α-$AnTe_3$[11,12] contains Te−Te single bonds and is charged balanced as $An^{4+}Te^{2-}Te_2^{2-}$. $AnTe_8$ bicapped trigonal prisms are the basic building blocks for the α-$AnTe_3$ structure where they are connected to each to other to form two-dimensional layers that are separated by a van der Waals gap. When these $AnTe_3$ layers

DOI: 10.1021/acs.inorgchem.5b00338
Inorg. Chem. 2015, 54, 3688−3694

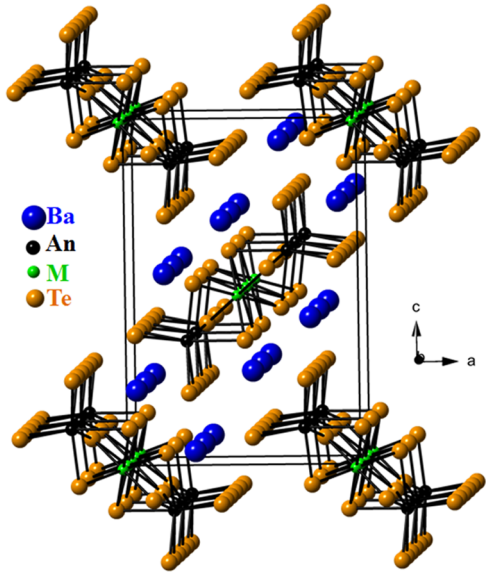

Figure 1. General view of the crystal structure of Ba_2TiUTe_7, Ba_2CrUTe_7, and $Ba_2CrThTe_7$ viewed along the *b*-axis. Here and in succeeding figures An (Th or U), Ba, M (Cr or Ti), and Te atoms are shown in black, blue, green, and orange, respectively.

combine with each other by sharing the Te atoms of Te−Te units, the three-dimensional UTe_2 structure results with infinite Te−Te−Te distances about 0.3 Å longer than a Te−Te single bond. Returning to α-$AnTe_3$, we find that flipping upside down one layer relative to the other creates the perfect octahedral positions for M atoms to fill and creates the $^1_\infty[MAnTe_7^{4-}]$ strips in Ba_2MAnTe_7. The fusion of these $^1_\infty[MAnTe_7^{4-}]$ strips generates the $^2_\infty[TiUTe_5^{1-}]$ layer in $CsTiUTe_5$.[18]

The U−Te interatomic distances (3.0818(4)−3.2839(1) Å) in Ba_2TiUTe_7 and Ba_2CrUTe_7 (Table 2) are in agreement with those in known related uranium tellurides (Table 3). The Th−Te distances in $Ba_2CrThTe_7$ are longer than the U−Te distances in Ba_2TiUTe_7 and Ba_2CrUTe_7 as a result of actinide contraction. The Th−Te distances compare favorably with those in known related thorium tellurides with eight coordinated thorium atoms (Table 4). The Ti−Te distances (2.8040(4)−2.8221(4) Å) in Ba_2TiUTe_7 can be compared with Ti^{2+}−Te distances in the charge balanced $Cs_2Ti_2U_6Te_{15}$ (2.787(1) Å)[42] and TiTe (2.730(1) Å) compounds.[43] However, Ti^{4+}−Te distances in $TiTe_2$ (2.770(1) Å),[44] $TiZrTe_4$ (2.754(1)−2.759(1) Å),[45] Cu_2TiTe_3 (2.647(1)−2.967(1) Å),[46] and $TlCuTiTe_3$ (2.678(4)−2.838(4) Å)[47] are close to these Ti^{2+}−Te distances where the Ti atom is also octahedrally coordinated. The Ti^{3+}−Te distances in $CsTi_5Te_8$ (2.7961(5)−2.8374(7) Å)[48] and $LiTiTe_2$ (2.804(1) Å)[49] are also comparable. Thus, it is not possible to assign an oxidation state to Ti in Ba_2TiUTe_7 on the basis of interatomic distances. The Cr−Te distances range from 2.7639(3) to 2.8191(3) Å in $Ba_2CrAnTe_7$ (An = Th, U) and are comparable with Cr^{3+}−Te distances in $CrTe_3$ (2.700(1)−2.755(1) Å),[50] Cr_2Te_3 (2.698(1)−2.778(1) Å),[51] $Cr_2Si_2Te_6$ (2.77(1)−2.80(1) Å),[52] $Cr_2Ge_2Te_6$ (2.769 (1)−2.819(3) Å),[53] $CrAuTe_4$ (2.7243(7)−2.7518(4) Å),[54] $TlCrTe_2$ (2.722(1) Å),[55] and $TlCr_5Te_8$ (2.691(1)−2.765(1) Å)[55] with the same Cr coordination. Among Cr/Te compounds, Cr^{3+} is very common when compared with the one known example of Cr^{2+}, namely CrTe where the Cr^{2+}−Te distance of 2.775(1) Å[56] is comparable with the Cr^{3+}−Te distances. Thus, the assignment of the oxidation state of Cr in Ba_2CrUTe_7 and $Ba_2CrThTe_7$ on the basis of interatomic distances is not possible.

Both barium atoms in these structures are connected to 10 Te atoms with Ba−Te interactions ranging from 3.4990(5) to 3.7508(5) Å. Compare these distances with those in $BaThTe_4$ (3.4545(7)−3.6315(7) Å),[17] $BaUTe_4$ (3.4334(7)−3.6136(11) Å),[17] $BaUTe_6$ (3.4927(7)−3.8195(7) Å),[17] and BaU_2Te_5 (3.574(1)−3.641(1) Å).[33]

It is interesting that Bond Valence Sum analysis,[57] as implemented in PLATON,[32] provided the following valences: Ba, 2.4−2.6; U, 3.1−3.2; Th, 4.0; Cr, 2.8−3.0; Ti, 3.4.The strictly empirical method depends for success on a large body of metrical

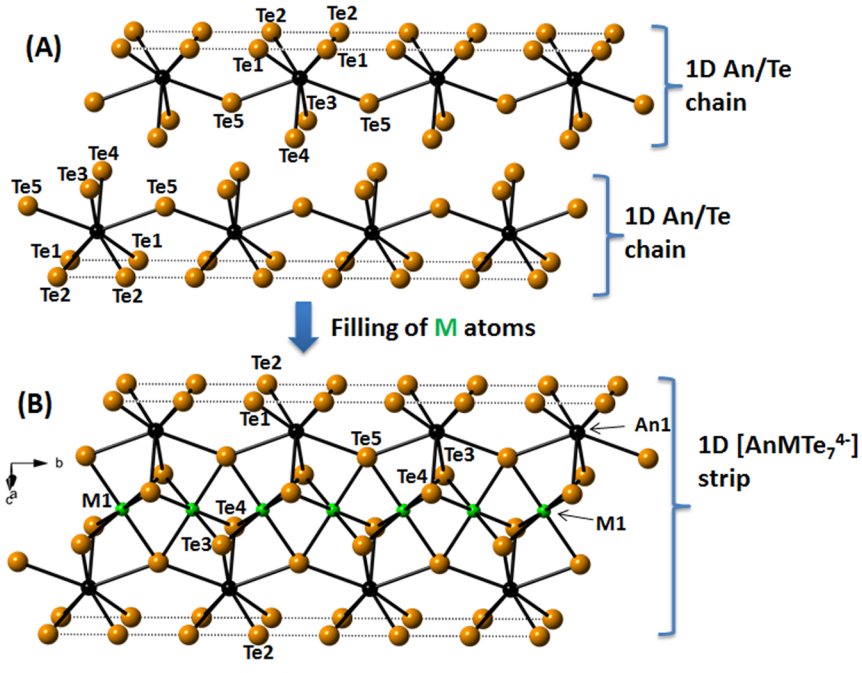

Figure 2. An and M network in the Ba_2MAnTe_7 structure formed by filling M atoms in between one-dimensional An/Te chains.

DOI: 10.1021/acs.inorgchem.5b00338
Inorg. Chem. 2015, 54, 3688−3694

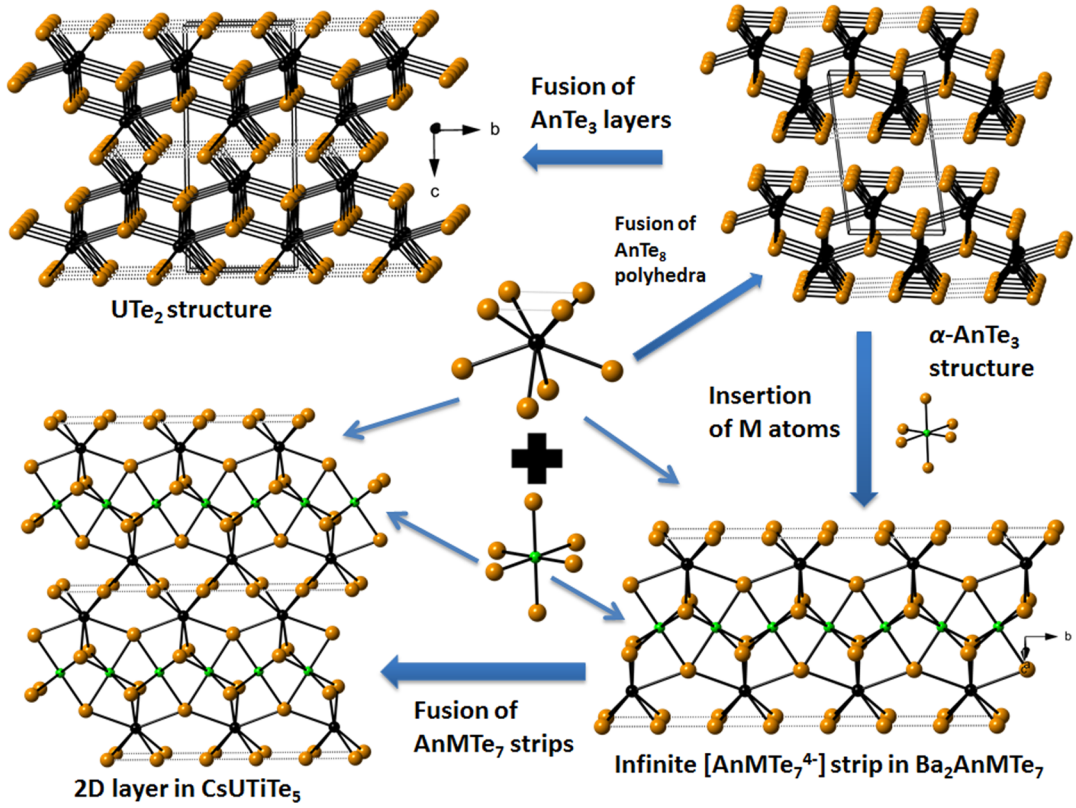

Figure 3. Relations among the Ba_2MAnTe_7, α-$AnTe_3$,[11,12] UTe_2,[13] and $CsTiUTe_5$[18] crystal structures.

Table 2. Selected Interatomic Lengths (Å) in the Ba_2MAnTe_7 Family

compd	Ba_2TiUTe_7	Ba_2CrUTe_7	$Ba_2CrThTe_7$
An1−Te1	3.1002(4) × 2	3.1042(3) × 2	3.1482(3) × 2
An1−Te2	3.1009(4) × 2	3.1026(3) × 2	3.1490(3) × 2
An1−Te3	3.1045(5) × 1	3.0914(4) × 1	3.1777(4) × 1
An1−Te4	3.0895(5) × 1	3.0818(4) × 1	3.1661(4) × 1
An1−Te5	3.2727(1) × 2	3.2839(1) × 2	3.3366(1) × 2
Ba1−Te1	3.5690(5) × 2	3.5636(4) × 2	3.5852(4) × 2
	3.6354(5) × 2	3.6311(4) × 2	3.6291(4) × 2
Ba1−Te2	3.5656(5) × 2	3.5674(4) × 2	3.5714(4) × 2
Ba1−Te3	3.7337(6) × 1	3.7038(5) × 1	3.7286(5) × 1
Ba1−Te4	3.5690(3) × 2	3.6125(3) × 2	3.6398(3) × 2
Ba1−Te5	3.4998(6) × 1	3.4990(5) × 1	3.5173(5) × 1
Ba2−Te1	3.6195(5) × 2	3.6135(4) × 2	3.6218(4) × 2
Ba2−Te2	3.5250(5) × 2	3.5471(4) × 2	3.5510(4) × 2
	3.5568(5) × 2	3.5274(4) × 2	3.5872(4) × 2
Ba2−Te3	3.5875(3) × 2	3.6292(3) × 2	3.6735(2) × 2
Ba2−Te4	3.7197(6) × 1	3.6962(5) × 1	3.7508(5) × 1
Ba2−Te5	3.5350(6) × 1	3.5321(5) × 1	3.5550(5) × 1
M1−Te3	2.8085(4) × 2	2.7639(3) × 2	2.7961(3) × 2
M1−Te4	2.8221(4) × 2	2.7716(3) × 2	2.8008(3) × 2
M1−Te5	2.8040(4) × 2	2.7831(3) × 2	2.8191(3) × 2
Te1···Te1	3.0542(6) × 1	3.0597(6) × 1	3.1012(5) × 1
Te1···Te1	3.0888(6) × 1	3.1056(6) × 1	3.1285(5) × 1
Te2···Te2	3.0460(6) × 1	3.0513(6) × 1	3.0959(5) × 1
Te2···Te2	3.0969(6) × 1	3.1140(6) × 1	3.1338(5) × 1
M1···M1	3.07147(5) × 2	3.083(1) × 2	3.115(1) × 2
An1···An1	6.143(1)	6.165(1)	6.230(1)

results. It does poorly here in the assignment of valences to the Ba atoms, and probably to the other atoms as well, perhaps owing to the paucity of metrical data involving such combinations of elements.

Oxidation States. Many actinide tellurides are notorious to charge balance owing to their propensity to form infinite linear Te−Te−Te chains. The present Ba_2MAnTe_7 compounds are no exception. These structures show intermediate Te−Te interactions (3.0460(6)−3.1338(5) Å) in the infinite Te−Te−Te chains. These intermediate Te−Te interactions are common among related actinide tellurides (Tables 3 and 4).

As noted above, the structural results in the present compounds are consistent with Th^{4+} and U^{4+}. For Ba_2TiUTe_7 with Ba^{2+} and U^{4+} consider the three most probable oxidation states for Ti, namely (a) Ti^{2+}, (b) Ti^{3+}, and (c) Ti^{4+}. With (a) the charges on the cations sum to 10; with (b) to 11; and with (c) to 12. Atoms Te3, Te4, and Te5 are free of Te−Te interactions and hence are each Te^{2-}. Thus, the charges on the remaining four Te atoms belonging to Te−Te−Te infinite chains are either (a) −1.0 (−4/4), (b) −1.25 (−5/4), or (c) −1.5 (−6/4) e^-. For (a), the Te−Te distance in the chains should be the single-bond distance of 2.76 Å, at least 0.3 Å shorter than observed. This leaves the possibility of Ti^{3+} or Ti^{4+}. The assumption of Ti^{4+} state in Ba_2TiUTe_7 would imply the presence of the Cr^{4+} state in isostructural $Ba_2CrAnTe_7$ (An = Th and U) which is rare in tellurides. On this basis Ti^{3+} seems more likely in Ba_2TiUTe_7, and this leads to an average charge of −1.25 e^- on each Te atom of the linear Te chain. In fact there are known Ti tellurides containing Ti^{3+}, for example $CsTi_5Te_8$[48] and $LiTiTe_2$. By implication $Ba_2CrAnTe_7$ (An = Th and U) would contain Cr^{3+}, which is the commonly occurring oxidation state in chromium tellurides, examples being $CrTe_3$,[50] Cr_2Te_3,[51] $Cr_2Ge_2Te_6$,[53] $CrAuTe_4$,[54] $TlCrTe_2$,[55] and $TlCr_5Te_8$.[55] Many actinide telluride structures are known that have infinite Te−Te−Te chains in which the Te−Te distances are of intermediate

DOI: 10.1021/acs.inorgchem.5b00338
Inorg. Chem. 2015, 54, 3688−3694

Table 3. U−Te and Te−Te Interactions in Some Related Compounds[a]

compound	structure	U−Te distances[b] (Å)	Te−Te (Å)	ref
Ba_2TiUTe_7	1-dimensional	3.0895(5)−3.2727(1)	3.0460(6)−3.0969(6)	this work
Ba_2CrUTe_7	1-dimensional	3.0818(4)−3.2839(1)	3.0513(6)−3.1140(6)	this work
BaU_2Te_5	layered	3.063(1)−3.219(1)		33
UTe_2	3-dimensional	3.076(1)−3.201(1)	3.057(1)−3.076(1)	13
$CsZrUTe_5$	layered	3.096(1)−3.360(1)	3.096(1)−3.112(1)	59
$CsTiUTe_5$	layered	3.059(1)−3.262(1)	3.065(1)	18
CsU_2Te_6	layered	3.089(1)−3.203(1)	2.989(1)−3.049(1)	15
$Tl_{0.56}UTe_3$	layered	3.093(2)−3.225(1)	3.037(1)−3.054(1)	60
$Cu_{0.78}U_2Te_6$	3-dimensional	3.100(1)−3.236(1)	3.029(1)−3.072(1)	20
$RbTiU_3Te_9$	3-dimensional	3.000(1)−3.216(1)	3.048(1)−3.051(1)	23
$CsTiU_3Te_9$	3-dimensional	2.966(3)−3.276(3)	3.051(1)−3.064(1)	23

[a]The U atom is coordinated to eight Te atoms in all of these structures. [b]Some entries have been rounded off to facilitate comparisons.

Table 4. Th−Te and Te−Te Interactions in Known Thorium Tellurides[a]

compound	structure	Th−Te (Å)	Te−Te (Å)	ref
$Ba_2CrThTe_7$	1-dimensional	3.1482(3)−3.3366(1)	3.0959(5)−3.1338(5)	this work
α-$ThTe_3$	layered	3.171(1)−3.250(1)	2.763(1)	11
Th_7Te_{12}	3-dimensional	3.137(2)−3.483(1)		61
$CuTh_2Te_6$	3-dimensional	3.165(1)−3.273(1)	3.058(1)−3.113(1)	19
KTh_2Te_6	layered	3.166(2)−3.264(1)	3.057(3)−3.085(3)	16
$CsTh_2Te_6$	layered	3.164(2)−3.264(2)	3.052(3)−3.088(3)	14
$MnThTe_3$	3-dimensional	3.160(1)−3.374(1)		21
$MgThTe_3$	3-dimensional	3.157(1)−3.374(1)		21
$BaThTe_4$	layered	3.199(1)−3.350(1)	2.766(1)−3.194(1)	17

[a]Some entries have been rounded off to facilitate comparisons.

length. Usually, noninteger charges on the Te atoms forming the infinite Te chains have been proposed as a somewhat arbitrary means of achieving charge balance. These include $BaAnTe_4$ (An = Th and U),[17] $CsAn_2Te_6$ (An = Th[14] and U[15]), KTh_2Te_6,[16] Cu_xUTe_3,[58] and $ATiU_3Te_9$ (A = Rb and Cs).[23]

Resistivity Studies. The high temperature-dependent resistivities for Ba_2TiUTe_7, Ba_2CrUTe_7, and $Ba_2CrThTe_7$ are shown in Figure 4. The resistivity of Ba_2CrUTe_7 decreases from

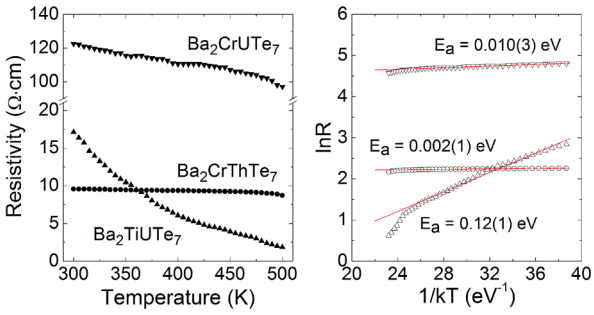

Figure 4. Resistivities and their corresponding Arrhenius plots for single crystals of Ba_2TiUTe_7, Ba_2CrUTe_7, and $Ba_2CrThTe_7$.

around 122 Ω cm at 300 K to about 100 Ω cm at 500 K, and resistivity for $Ba_2CrThTe_7$ decreases from around 10 Ω cm at 300 K to about 9 Ω cm at 500 K. These nearly temperature-independent resistivities are consistent with very narrow semiconducting behaviors with activation energies of 10(3) meV and 2(1) meV for Ba_2CrUTe_7 and $Ba_2CrThTe_7$, respectively. Ba_2TiUTe_7 shows a much stronger temperature dependence with a decreasing resistivity of around 17 Ω cm at 300 K to 2 Ω cm at 500 K. The activation energy for semiconducting Ba_2TiUTe_7 was calculated to be 0.12(1) eV from the corresponding Arrhenius plot. For Ba_2TiUTe_7, the region between 460 and 500 K shows a different linear trend from that between 300 and 460 K. This may indicate a change in the mechanism of carrier activation.

DFT Calculations. The computed total and partial density of states for Ba_2TiUTe_7 and Ba_2CrUTe_7 are presented in Figures 5 and 6, respectively. As seen from the total density of states (upper plots), both compounds have vanishing density of states at the Fermi level. Therefore, they are either poor metals or semiconductors with a very small gap. Concerning $Ba_2CrThTe_7$, we found it to be an antiferromagnet (as seen from its totally symmetric total density of states), with most of the spin polarization carried by the Cr atoms while the Th atoms carry a negligible magnetic moment. The magnetic moment of the Cr atoms induces a small magnetic polarization on the other atoms, as best seen from the partial density of states of atoms Te3, Te4, and Te5. Also, the states around the Fermi level mainly comprise Cr-d and Th-f orbitals. Ba_2TiUTe_7 is found to be a ferromagnet with a magnetic moment carried by the U atoms, with a weaker magnetic moment on the Ti atoms. As for $Ba_2CrThTe_7$, a small spin polarization is induced on the other atoms, and the states around the Fermi level correspond to U-f states.

CONCLUSIONS

Three new quaternary actinide tellurides Ba_2TiUTe_7, Ba_2CrUTe_7, and $Ba_2CrThTe_7$ were obtained by reaction of elements at 1173 K. Single-crystal X-ray diffraction studies show that these three compounds are isostructural and crystallize in a new structure type in the orthorhombic system in space group D_{2h}^{16}−*Pnma* with four formula units per cell. The asymmetric unit of these structures is composed of one An atom (site symmetry .*m*.), two Ba atoms (.*m*.), one M atom ($\bar{1}$), and five Te atoms (Te1(1), Te2(1) Te3(.*m*.), Te4(.*m*.), and Te5(.*m*.)). Each An

DOI: 10.1021/acs.inorgchem.5b00338
Inorg. Chem. 2015, 54, 3688−3694

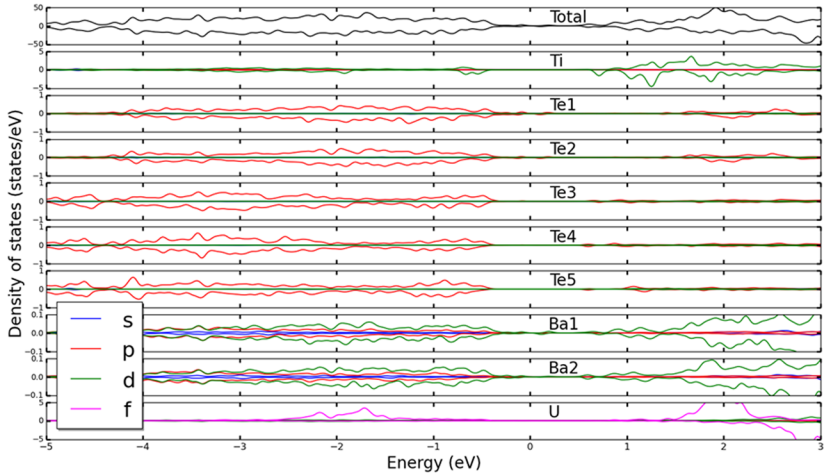

Figure 5. Total (upper plot) and partial density of states (lower plots) of Ba_2TiUTe_7.

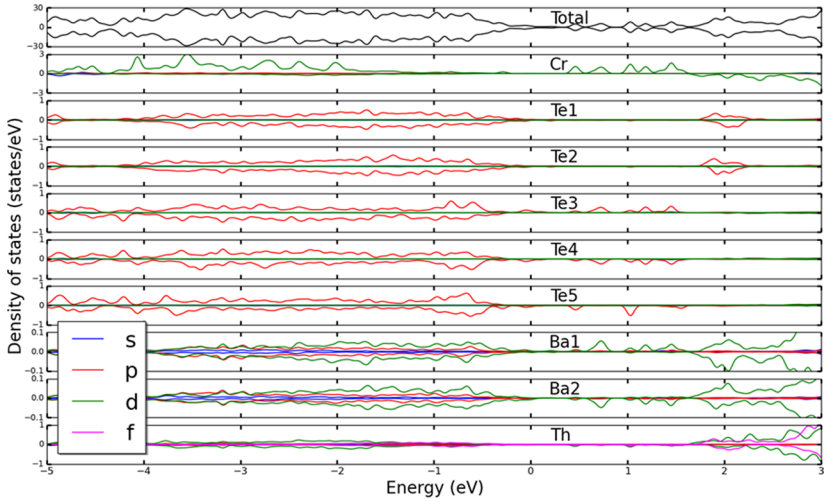

Figure 6. Total (upper plot) and partial density of states (lower plots) of $Ba_2CrThTe_7$.

atom in this structure is coordinated to eight Te atoms in a bicapped trigonal-prismatic arrangement and each M atom is octahedrally coordinated to six Te atoms. Sharing of the $AnTe_8$ and MTe_6 polyhedra results in formation of $1[MAnTe_7^{4-}]$ strips that also feature infinite linear Te−Te−Te chains with intermediate Te−Te interactions. These $1[MAnTe_7^{4-}]$ strips propagate along the *b*-axis and are separated by Ba cations. Assignment of formal charges in these compounds is arbitrary owing to the presence of these infinite Te−Te−Te chains. High temperature-dependent resistivity measurements indicate that these compounds are narrow band gap semiconductors. At 300 K the resistivities are 17, 122, and 10 Ω cm for Ba_2TiUTe_7, Ba_2CrUTe_7, and $Ba_2CrThTe_7$, respectively. Poor metallic or semiconducting behavior (with narrow band gaps) for Ba_2TiUTe_7 and $Ba_2CrThTe_7$ is predicted by DFT calculations corroborating the resistivity measurements. The theoretical calculations also predict that Ba_2TiUTe_7 is ferromagnetic and $Ba_2CrThTe_7$ is antiferromagnetic.

■ ASSOCIATED CONTENT

Supporting Information

Crystallographic file in cif format for Ba_2TiUTe_7, Ba_2CrUTe_7, and $Ba_2CrThTe_7$. This material is available free of charge via the Internet at http://pubs.acs.org

■ AUTHOR INFORMATION

Corresponding Author

*E-mail: ibers@chem.northwestern.edu.

Notes

The authors declare no competing financial interest.

■ ACKNOWLEDGMENTS

Use was made of the IMSERC X-ray Facility at Northwestern University, supported by the International Institute of Nanotechnology (IIN). S.L. acknowledges HPC resources from GENCI-CCRT/CINES (Grant x2014-085106).

■ REFERENCES

(1) Damien, D.; de Novion, C. H.; Gal, J. *Solid State Commun.* **1981**, *38*, 437−440.
(2) de Novion, C. H.; Damien, D.; Hubert, H. *J. Solid State Chem.* **1981**, *39*, 360−367.
(3) *The Actinides: Electronic Structure and Related Properties*; Freeman, A. J., Darby, J. B., Jr., Eds.; Academic Press: New York, 1974; Vol. *1, 2*.
(4) Bugaris, D. E.; Ibers, J. A. *Dalton Trans.* **2010**, *39*, 5949−5964.
(5) Manos, E.; Kanatzidis, M. G.; Ibers, J. A. In *The Chemistry of the Actinide and Transactinide Elements*, 4th ed.; Morss, L. R., Edelstein, N. M., Fuger, J., Eds.; Springer: Dordrecht, The Netherlands, 2010; Vol. *6*, pp 4005−4078.

DOI: 10.1021/acs.inorgchem.5b00338
Inorg. Chem. 2015, 54, 3688−3694

(6) Choi, K.-S.; Patschke, R.; Billinge, S. J. L.; Waner, M. J.; Dantus, M.; Kanatzidis, M. G. *J. Am. Chem. Soc.* **1998**, *120*, 10706−10714.
(7) Riley, B. J.; Chun, J.; Um, W.; Lepry, W. C.; Matyas, J.; Olszta, M. J.; Li, X.; Polychronopoulou, K.; Kanatzidis, M. G. *Environ. Sci. Technol.* **2013**, *47*, 7540−7547.
(8) Manos, M. J.; Kanatzidis, M. G. *J. Am. Chem. Soc.* **2009**, *131*, 6599−6607.
(9) Manos, M. J.; Kanatzidis, M. G. *Chem.—Eur. J.* **2009**, *15*, 4779−4784.
(10) Mertz, J.; Fard, Z. H.; Malliakas, C. M.; Manos, M. J.; Kanatzidis, M. G. *Chem. Mater.* **2013**, *25*, 2116−2127.
(11) Prakash, J.; Ibers, J. A. *Z. Anorg. Allg. Chem.* **2014**, *640*, 1943−1945.
(12) Stöwe, K. *Z. Anorg. Allg. Chem.* **1996**, *622*, 1419−1422.
(13) Beck, H. P.; Dausch, W. *Z. Naturforsch., B: Chem. Sci.* **1988**, *43*, 1547−1550.
(14) Cody, J. A.; Ibers, J. A. *Inorg. Chem.* **1996**, *35*, 3836−3838.
(15) Mesbah, A.; Ibers, J. A. *Acta Crystallogr., Sect. E: Struct. Rep. Online* **2012**, *68*, i76.
(16) Wu, E. J.; Pell, M. A.; Ibers, J. A. *J. Alloys Compd.* **1997**, *255*, 106−109.
(17) Prakash, J.; Lebègue, S.; Malliakas, C. D.; Ibers, J. A. *Inorg. Chem.* **2014**, *53*, 12610−12616.
(18) Cody, J. A.; Ibers, J. A. *Inorg. Chem.* **1995**, *34*, 3165−3172.
(19) Narducci, A. A.; Ibers, J. A. *Inorg. Chem.* **1998**, *37*, 3798−3801.
(20) Huang, F. Q.; Ibers, J. A. *J. Solid State Chem.* **2001**, *159*, 186−190.
(21) Narducci, A. A.; Ibers, J. A. *Inorg. Chem.* **2000**, *39*, 688−691.
(22) Bugaris, D. E.; Ibers, J. A. *J. Solid State Chem.* **2009**, *182*, 2587−2590.
(23) Ward, M. D.; Mesbah, A.; Lee, M.; Malliakas, C. D.; Choi, E. S.; Ibers, J. A. *Inorg. Chem.* **2014**, *53*, 7909−7915.
(24) Bugaris, D. E.; Ibers, J. A. *J. Solid State Chem.* **2008**, *181*, 3189−3193.
(25) Haneveld, A. J. K.; Jellinek, F. *J. Less-Common Met.* **1969**, *18*, 123−129.
(26) Murasik, A.; Suski, W.; Leciejewicz, J. *Phys. Status Solidi* **1969**, *34*, K157−K158.
(27) Beck, H. P.; Dausch, W. *Z. Anorg. Allg. Chem.* **1989**, *571*, 162−164.
(28) *Bruker APEX2 Version 2009.5−1 Data Collection and Processing Software*; Bruker Analytical X-Ray Instruments, Inc.: Madison, WI, 2009.
(29) Sheldrick, G. M. *SADABS*; Department of Structural Chemistry, University of Göttingen: Göttingen, Germany, 2008.
(30) Sheldrick, G. M. *Acta Crystallogr., Sect. A: Found. Crystallogr.* **2008**, *64*, 112−122.
(31) Gelato, L. M.; Parthé, E. *J. Appl. Crystallogr.* **1987**, *20*, 139−143.
(32) Spek, A. L. *PLATON, A Multipurpose Crystallographic Tool*; Utrecht University: Utrecht, The Netherlands, 2014.
(33) Prakash, J.; Tarasenko, M. S.; Mesbah, A.; Lebègue, S.; Malliakas, C. D.; Ibers, J. A. *Inorg. Chem.* **2014**, *53*, 11626−11632.
(34) Kresse, G.; Forthmüller, J. *Comput. Mater. Sci.* **1996**, *6*, 15−50.
(35) Kresse, G.; Joubert, D. *Phys. Rev. B* **1999**, *59*, 1758−1775.
(36) Kohn, W.; Sham, L. J. *Phys. Rev.* **1965**, *140*, 1133−1138.
(37) Hohenberg, P.; Kohn, W. *Phys. Rev.* **1964**, *136*, 864−871.
(38) Blöchl, P. E. *Phys. Rev. B* **1994**, *50*, 17953−17979.
(39) Heyd, J.; Scuseria, G. E.; Ernzerhof, M. *J. Chem. Phys.* **2003**, *118*, 8207−8215.
(40) Heyd, J.; Scuseria, G. E.; Ernzerhot, M. *J. Chem. Phys.* **2006**, *124*, 219906−1.
(41) Paier, J.; Marsman, M.; Hummer, K.; Kresse, G.; Gerber, I. C.; Angyan, J. G. *J. Chem. Phys.* **2006**, *124*, 154709.
(42) Ward, M. D.; Oh, G. N.; Mesbah, A.; Lee, M.; Choi, E. S.; Ibers, J. A. *J. Solid State Chem.* **2015**, submitted.
(43) Oudet, X. *Ann. Chim.* **1983**, *8*, 483−505.
(44) Arnaud, Y.; Chevreton, M. *J. Solid State Chem.* **1981**, *39*, 230−239.
(45) Cybulski, Z.; Feltz, A.; Andratschke, M. *Mater. Res. Bull.* **1989**, *24*, 157−162.
(46) Bensch, W.; Dürichen, P. *Z. Kristallogr.* **1994**, *209*, 687.
(47) Pell, M. A.; Ibers, J. A. *J. Alloys Compd.* **1996**, *240*, 37−41.
(48) Gray, D. L.; Ibers, J. A. *J. Alloys Compd.* **2007**, *440*, 74−77.
(49) Patel, S. N.; Balchin, A. A. *J. Mater. Sci. Lett.* **1985**, *4*, 382−384.
(50) Canadell, E.; Jobic, S.; Brec, R.; Rouxel, J. *J. Solid State Chem.* **1992**, *98*, 59−70.
(51) Hamasaki, T.; Hashimoto, T.; Yamaguchi, Y.; Watanabe, H. *Solid State Commun.* **1975**, *16*, 895−897.
(52) Ouvrard, G.; Sandre, E.; Brec, R. *J. Solid State Chem.* **1988**, *73*, 27−32.
(53) Carteaux, V.; Brunet, D.; Ouvrard, G.; Andre, G. *J. Phys.: Condens. Matter* **1995**, *7*, 69−87.
(54) Reynolds, T. K.; McGuire, M. A.; DiSalvo, F. J. *J. Solid State Chem.* **2004**, *177*, 2998−3006.
(55) Boller, H.; Klepp, K. O.; Kirchmayr, K. *Mater. Res. Bull.* **1995**, *30*, 365−371.
(56) Makovetskii, G. I.; Galyas, A. I.; Severin, G. M.; Yanushkevich, K. I. *Inorg. Mater. (Transl. of Neorg. Mater.)* **1996**, *32*, 846−849.
(57) Brown, I. D. *The Chemical Bond in Inorganic Chemistry, The Bond Valence Model*; Oxford University Press: New York, 2002.
(58) Patschke, R.; Breshears, J. D.; Brazis, P.; Kannewurf, C. R.; Billinge, S. J. L.; Kanatzidis, M. G. *J. Am. Chem. Soc.* **2001**, *123*, 4755−4762.
(59) Kim, J.-Y.; Gray, D. L.; Ibers, J. A. *Acta Crystallogr., Sect. E: Struct. Rep. Online* **2006**, *E62*, i124−i125.
(60) Tougait, O.; Daoudi, A.; Potel, M.; Noël, H. *Mater. Res. Bull.* **1997**, *32*, 1239−1245.
(61) Tougait, O.; Potel, M.; Noël, H. *Inorg. Chem.* **1998**, *37*, 5088−5091.

DOI: 10.1021/acs.inorgchem.5b00338
Inorg. Chem. 2015, 54, 3688−3694